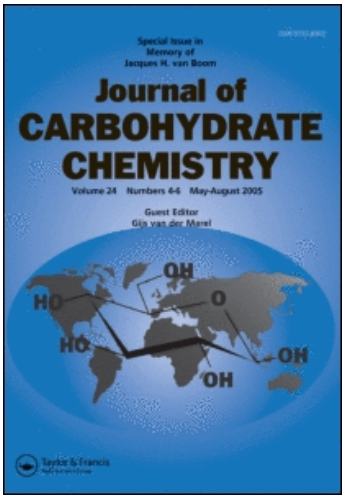

Journal of Carbohydrate Chemistry

Publication details, including instructions for authors and subscription information:
http://www.informaworld.com/smpp/title~content=t713617200

The Conformation of the Tri- and Tetrasaccharide Produced in the Hydrolysis of Barley Glucan with the Enzyme Endo-1,3-1,4-β-glucan 4-Glucanohydrolase from *Bacillus Licheniformis*

M. Bernabé[a]; J. Jiménez-Barbero[a]; A. Planas[b]
[a] Grupo de Carbohidratos, Instituto de Química Orgánica General (CSIC), Madrid, Spain [b] CETS Institut Químic de Sarriá, Universitat Ramón Llull, Barcelona, Spain

To cite this Article Bernabé, M. , Jiménez-Barbero, J. and Planas, A.(1994) 'The Conformation of the Tri- and Tetrasaccharide Produced in the Hydrolysis of Barley Glucan with the Enzyme Endo-1,3-1,4-β-glucan 4-Glucanohydrolase from *Bacillus Licheniformis*', Journal of Carbohydrate Chemistry, 13: 5, 799 — 817
To link to this Article: DOI: 10.1080/07328309408011681
URL: http://dx.doi.org/10.1080/07328309408011681

J. CARBOHYDRATE CHEMISTRY, 13(5), 799-817 (1994)

THE CONFORMATION OF THE TRI- AND TETRASACCHARIDE PRODUCED IN THE HYDROLYSIS OF BARLEY GLUCAN WITH THE ENZYME ENDO-1,3-1,4-ß-GLUCAN 4-GLUCANOHYDROLASE FROM *BACILLUS LICHENIFORMIS*

M. Bernabé, J. Jiménez-Barbero,* and A. Planas[a]

Grupo de Carbohidratos, Instituto de Química Orgánica General (CSIC), Juan de la Cierva 3, 28006 Madrid (Spain)
[a]CETS Institut Químic de Sarriá, Universitat Ramón Llull, 08017-Barcelona (Spain)

Received April 24, 1993 - Final Form February 15, 1994

ABSTRACT

The solution conformation of the tri- and tetrasaccharide obtained by enzymatic degradation of glucan has been analysed using molecular mechanics and dynamics calculations and nuclear magnetic resonance data. The overall shape of both compounds is fairly similar and may be described by an equilibrium formed by conformers included in the low energy regions for both glycosidic linkages. The interglycosidic torsion angles for these conformers are Φ_H=15±45° and Ψ_H= -20±30° for both β(1->4) linkages and Φ_H=40±15° and Ψ_H= -20±35° for the corresponding ß(1->3)-linked moiety.

INTRODUCTION

The depolymerization of poly-ß-glucans is catalysed by a number of enzymes, ß-D-glucanases, which differ in their substrate specificity and cleavage pattern. Barley ß-glucan is known to be a linear polysaccharide of ß-(1->4) and ß-(1->3) linkages in a 2.5 to 1 ratio.[1] Hydrolysis with endo-1,3-1,4-ß-glucan 4-glucanohydrolase (E.C.3.2.1.73) yields 3-ß-*O*-cellobiosyl-D-glucopyranose (1) and 3-ß-*O*-

cellotriosyl-D-glucopyranose (**2**) as final products,[1a] defining the cleavage specificity as ß-(1->4) glycosidic linkages on 3-*O*-substituted glucopyranose units. This enzyme is of current interest because of its application in carbohydrate technology,[2] and fundamental research mainly directed to microbial isozymes. The structures of the tri- and tetrasaccharides **1** and **2** produced by treatment of barley ß-glucan with recombinant *endo*-1,3-1,4-ß-glucan 4-glucanohydrolase from *Bacillus licheniformis* have been confirmed in our group by assignment of their NMR data.[3] The enzymic hydrolysis has been determined to proceed with retention of configuration at the anomeric centers as shown by ^{1}H NMR monitoring of the reaction.[3] The recently solved three-dimensional structure of a hybrid ß-glucanase by X-ray crystallography[4] will provide valuable information on the active site geometry. The protein structure has been determined at 2.0 Å resolution for the free enzyme, and at 2.8 Å for a covalent protein-inhibitor complex with 3,4-epoxybutyl-ß-D-cellobioside. Although this molecule is an active-site directed inhibitor,[5] its structure only resembles partially the natural substrate, since its aglycon moiety interacting with catalytic residues is an extended hydrocarbon chain. In order to further study the enzyme-substrate interactions by molecular modelling techniques, we here analyse the solution conformation of both **1** and **2**, using molecular mechanics and dynamics calculations, and NMR (NOE) data. Similar but different oligosaccharide structures have been reported to be isolated by degradation of barley ß-glucan with an *Aspergillus niger* ß-glucanase.[6] In that work, one trisaccharide and two tetrasaccharides were obtained along with a hexasaccharide. However, the trisaccharide was found to have the opposite alternation of ß-(1->4) and ß-(1->3) linkages: ß-Glc*p*-(1->3)-ß-Glc*p*-(1->4)-Glc*p*-, while the tetrasaccharides had also different primary sequences and were identified as ß-Glc*p*-(1->4)-ß-Glc*p*-(1->3)-Glc*p*-ß-(1->4)-Glc*p*, and ß-Glc*p*-(1->3)-ß-Glc*p*-(1->4)-Glc*p*-ß-(1->4)-Glc*p*.

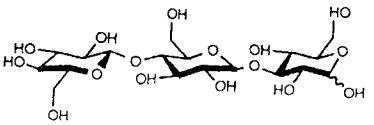

1

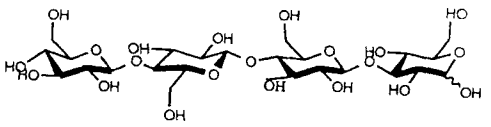

2

TABLE I

Estimated Populations (%) for the low energy conformers of **1** and **2**, estimated from the AMBER[a] and CVFF[b] steric energy values.($\Phi = \Phi_H$-120°, $\Psi = \Psi_H$-120°).

ß(1->4)	Conformer Φ_H/Ψ_H(°)[c]				
	(A)55/5	(B)30/-50	(C) -30/-30	(D)175/0	(E)55/180
POP. Φ_3/Ψ_3[a]	38	34	26	2	<1
POP. Φ_2/Ψ_2	43	34	22	2	<1
POP. Φ_3/Ψ_3[b]	40	33	25	2	<1
POP. Φ_2/Ψ_2	48	31	20	1	<1
ß(1->3)	Conformer Φ_H/Ψ_H(°)[c]				
	(A')55/15	(B')35/-55	(C') -30/-30	(D')70/60	(E') 170/5
POP. Φ_1/Ψ_1[a]	55	39	4	2	<1
POP. Φ_1/Ψ_1[b]	63	32	4	1	<1

a. AMBER energy values. b. CVFF energy values. c. Glycosidic angles are given using hydrogens as reference. The torsion angle values for the different local minima A-E when using either the AMBER or the CVFF force fields did not differ more than 10° from these figures. The populations are calculated from the energy values for the corresponding local minima and not for the conformers having the exact Φ/Ψ value.

RESULTS AND DISCUSSION

Table I shows the values of the estimated populations of the low energy conformers of **1** and **2** obtained by CVFF optimisation of the possible geometries previously reported for the component disaccharides. The use of the AMBER program produced fairly similar results. Due to the presence of a number of electronegative atoms, these energies should be taken as approximate since they are variable at least 0.5 Kcal/mol. There are broad low energy regions in both cases, along with small islands populated by conformers with a rather different ϕ,Ψ angle.[7,8] The previously reported X-ray structures for different β(1->4) and β(1->3) equatorial linked dissacharides are included in this low energy region.[9] According to the calculations, the low energy region for the β(1->4) linkage is described by Φ_H=15±45°, Ψ_H=-20±30°, and r_{H}-1'-H-4=2.4±0.3Å appears to be populated in more than 90% extent while the two

minor islands described by conformers D and E are populated less than 5% at 40 °C, as estimated in different conformational studies of ß(1->4) equatorial-linked disaccharides.[7,8,10] Nevertheless, the possibility of their existence in solution can not be discarded *a priori* since the conformation of some interglycosidic acetals synthesized from lactose and cellobiose[11] is that of conformer D, while the recent X-ray analysis of the bound conformation of a biantennary octasaccharide to *Lathyrus Ochrus Isolectin I* has shown the existence of a Man β(1->4) GlcNAc linkage in conformation E, and a Gal β(1->4)GlcNac moiety located in island D.[12] On the other hand, the low energy region for the β(1->3) glycosidic linkage is described by Φ_H=45±25°, Ψ_H=5±55°. The X-ray structures of different laminaribiose derivatives included in this low energy region mainly differ in the value of Ψ angle.[9] The conformational stability of the different conformers was studied by using MD simulations with the Discover-CVFF and the Discover-AMBER programmes. Although these are general MD programmes not specifically parametrized for carbohydrates,[13] and therefore do not include any extra potential to account for the *endo-* or *exo*-anomeric effects,[14] its use in the conformational study of different oligosaccharides has produced satisfactory results.[15] All the different conformations were used as input geometries for independent 1 ns simulations at 313 °K. The trajectories of some of them are displayed in Figure 1a. In all cases, no chair to chair or chair to boat interconversions were observed. The average Φ_H and Ψ_H angles were calculated to be 15±30° and -30±20° for the ß(1->4) linkages, and 40±10° and -15±20° for the ß(1->3), depending on the starting conformer. It can be observed that the trajectories remained most of the time (>90%) in the broad regions. In fact, only when the calculation started from E-type minima for the ß(1->4) linkage, the trajectories spent a fraction of time within these islands (*ca.* 200 ps), although the trajectory went again to the main low energy region. Also when the starting geometry was that of conformer D, the simulation resulted in a transition to region A-C within a few picoseconds. In addition, the low-energy region, around conformers A and B, satisfies the geometric requirements for the occurrence of the *exo*-anomeric effect. Therefore, with regard to the ß(1->4) linkages, these results seem to indicate that minima D and E are not stable enough in comparison to conformers A-C',[16] when external factors such as stabilization by hydrogen or covalent bonds or non polar contacts are not involved.[12] In the case of the ß(1->3) linkage, the trajectory spent most of the time in the region of conformer A', which according to both CVFF and AMBER programs seems to be more stable than minimum B', although this is predicted to be slightly predominant by MM3 calculations.[8] Moreover, the region around conformer A' would also be additionally stabilised by the *exo*-anomeric effect.

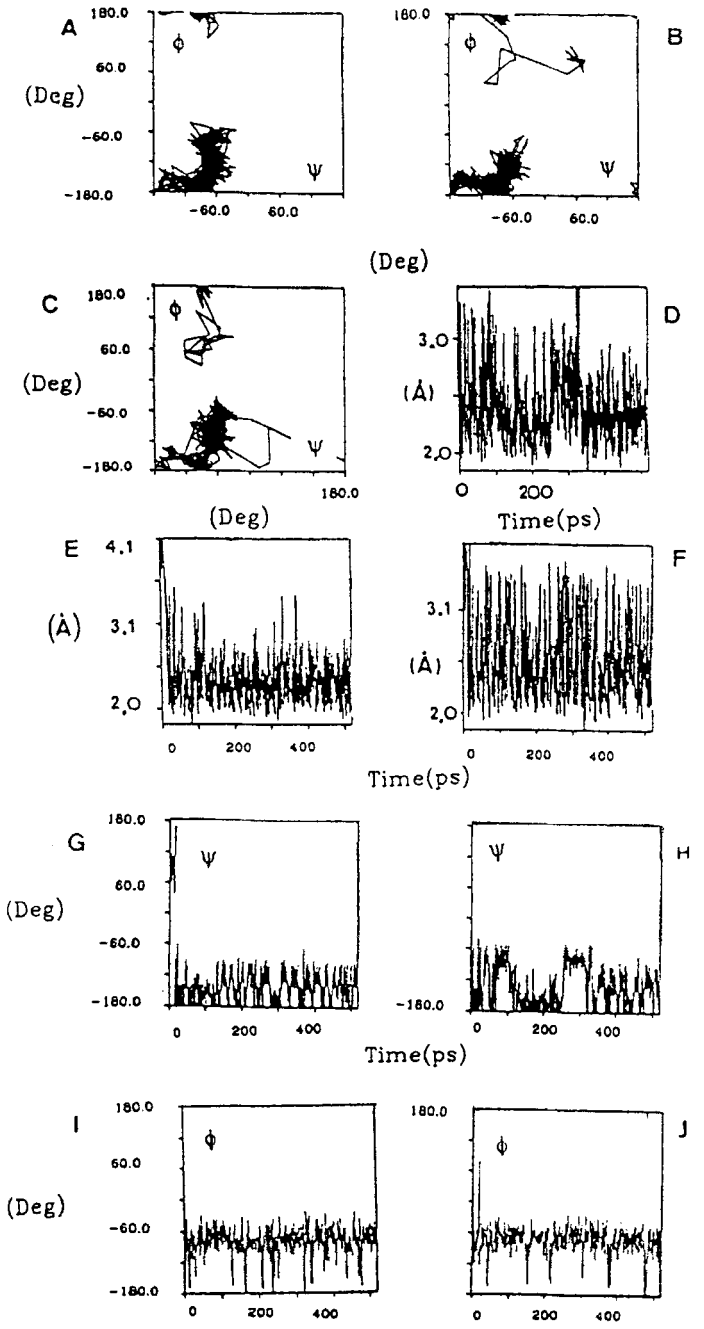

Figure 1a. 2D and 1D plots of the of the MD trajectories, and history of the relevant interatomic distances (Å), calculated by the CVFF programme for **2** at 313 °K . (A) Trajectory plot for Φ_3/Ψ_3 torsion angles (°). (B) Trajectory plot for Φ_2/Ψ_2 angles (°). (C) Trajectory plot for Φ_1/Ψ_1 angles (°). (D) History of $r_{H1'''\text{-}H\text{-}4''}$ distance (Å). (E) History of $r_{H1''\text{-}H\text{-}4'}$ distance (Å). (F) History of $r_{H1'\text{-}H\text{-}4}$ distance (Å). (G) History of Ψ_3 *angle*(°). (H) History of Ψ_1 angle(°). (I) History of Φ_3 angle(°).(J) History of Φ_1 angle(°).

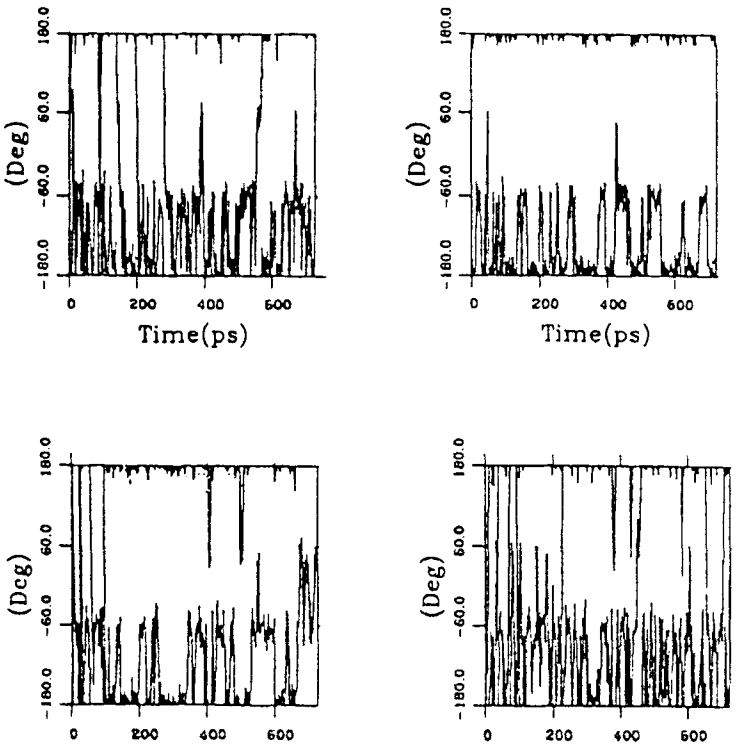

Figure 1b. 1D trajectory plots of the of the MD trajectories of the lateral chains of the glucopyranose residues of **2**. Transitions between the *gg* (180°) and the *gt* (-60°) rotamers can be observed for all the residues. The occupance of the *tg* region (60°) is almost negligible.

The two other local minima (C', D') present in the low energy region, and those located in islands do not appear to be stable. In all cases, several transitions between the favored orientations of the C-5-C-6 chains (*gg* and *gt*) were observed, as depicted in Figure 1b.

NMR spectroscopy may be used to distinguish the presence of either conformer.[17,18] All the low energy region for the ß(1->4) linkage is described by short distances between H-4' and H-1'', while H-3' is close to H-1'' in conformer E, H-4 'close to H-2'' in conformer D, and there is an unique contact between H-1'' and H-6'$_{proR}$ or H-6'$_{proS}$ for the *gg* or *gt* rotamers of conformer A, respectively. In the case of the ß(1->3) linkage, the low energy region is described by A' and B' conformers with short distances between H-3 and H-1', H-3 is also close to H-1' in conformer C', and H-2 close to H-1' in conformer D'. In addition, conformers A and B of the ß(1->4) linkage can be stabilized by intramolecular hydrogen bond between HO-3 and O-5' since

TABLE II
Relevant interatomic distances for the low energy conformers of **1** and **2**.

Distance(Å)	Conformer(Φ_H/Ψ_H)				
ß(1->4)	Conformer Φ_H/Ψ_H(°)				
	(A)55/5	(B)30/-50	(C) -30/-30	(D)175/0	(E)55/180
H-1''-H-4'	2.33	2.34	2.23	>3.5	>3.5
H-1''-H-3'	>3.5	>3.5	>3.5	>3.5	1.79
H-1''-H-5'	>3.5	>3.5	>3.5	>3.5	2.23
H-1''-H-6'$_R$	2.49[a]	>3.5	>3.5	>3.5	>3.5
H-1''-H-6'$_S$	2.62[b]	>3.5	>3.5	>3.5	>3.5
H-1''-O-3'	>3.5	2.48	2.47	>3.5	>3.5
H-1''-O-6'	2.52	>3.5	>3.5	>3.5	>3.5
H-2''-H-4'	>3.5	>3.5	>3.5	1.94	>3.5
O-2''-O-3'	>3.5	>3.5	>3.5	2.93	>3.5
O-5''-O-3'	3.02	2.63	3.06	>3.5	>3.5
O-2''-H-6'$_R$	2.96[a]	>3.5	3.12	>3.5	>3.5
O-2''-H-6'$_S$	2.99[b]	>3.5	3.06	>3.5	>3.5
ß(1->3)	Conformer Φ_H/Ψ_H(°)				
	(A')55/15	(B')35/-50	(C') -30/-30	(D')70/60	
H-1'-H-4	2.49	2.24	2.23	3.18	
H-1'-H-3	>3.5	>3.5	>3.5	>3.5	
H-1'-H-2	>3.5	>3.5	>3.5	2.71	
H-1'-O-4	>3.5	2.58	2.37	>3.5	
H-1'-O-2	2.72	>3.5	>3.5	2.08	
O-5'-O-4	3.32	2.16	>3.5	>3.5	

a. *gg* conformer for the lateral chain. b. *gt* conformer. $\Phi = \Phi_H - 120°$, $\Psi = \Psi_H - 120°$

TABLE III
^{1}H NMR chemical shifts (δ , ppm) for **1** and **2** in D_2O solution at 40 °C.

Unit		H-1	H-2	H-3	H-4	H-5	H-6A	H-6B
Trisaccharide 1								
ß-D-Glcp	C	4.50	3.31	3.50	3.41	3.49	3.91	3.73
4-O-ß-D-Glcp	B	4.75	3.40	3.67	3.66	3.63	3.98	3.81
3-O-ß-D-Glcp	Aα	5.23	3.72	3.90	3.52	3.87	3.89	3.76
	Aß	4.66	3.43	3.75	3.52	3.50	3.91	3.73
Tetrasaccharide 2								
ß-D-Glcp	D	4.51	3.32	3.52	3.43	3.51	3.93	3.75
4-O-ß-D-Glcp	C	4.54	3.40	3.70	3.70	3.67	4.02	3.86
4-O-ß-D-Glcp	B	4.76	3.41	3.69	3.69	3.65	4.01	3.85
3-O-ß-D-Glcp	Aα	5.24	3.74	3.92	3.54	3.89	3.88	3.78
	Aß	4.67	3.46	3.76	3.53	3.52	3.92	3.75

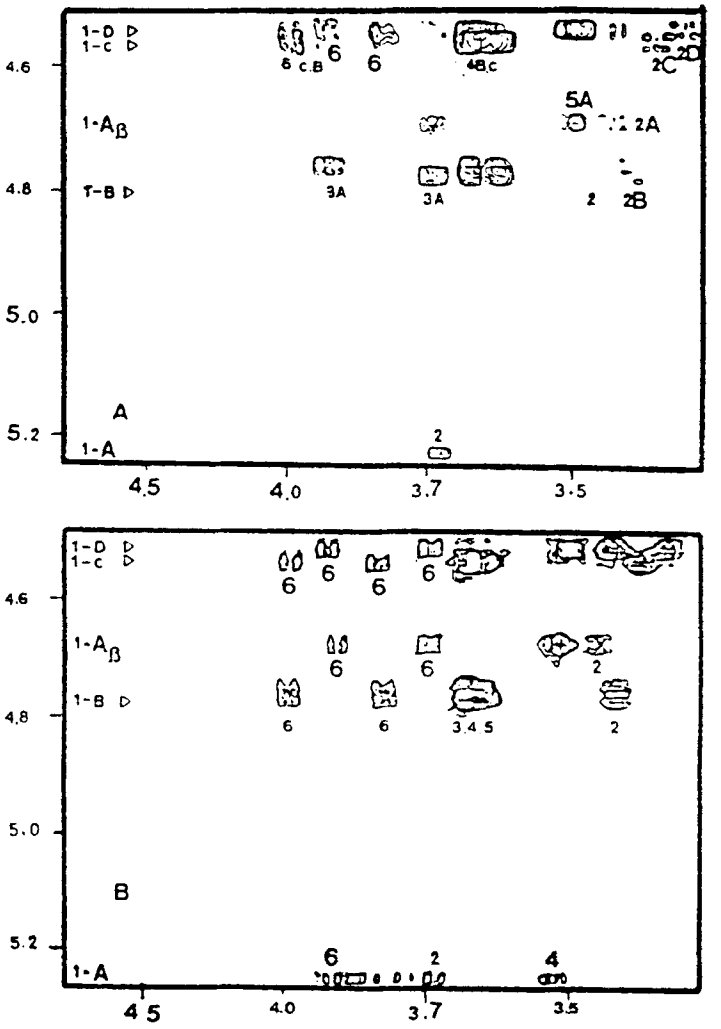

Figure 2. ROESY (A, above) and TOCSY (B, below) cross peaks for the anomeric protons of **2**. Relevant connectivities are indicated.

both oxygen atoms are less than 3.0 Å apart. The same situation is held between HO-4 and O-5' of conformer B' for the ß(1->3) linkage. These structural characteristics are shown in Table II. The observation of one or two interresidue NOEs and some specific shieldings or deshieldings can impose constraints in the energy map to assess the existence of a given conformation. The previous step for the analysis of the NOE data was the assignment of the different resonances through a combination of 2D-NMR techniques,

TABLE IV
^{13}C NMR chemical shifts (δ , ppm) for 1 and 2 in D_2O solution at 40 °C.

Unit		C-1	C-2	C-3	C-4	C-5	C-6
Trisaccharide 1							
ß-D-Glcp	C	103.4	74.1	76.5	70.4	76.9	61.6
4-O-ß-D-Glcp	B	103.5	74.2	75.1	79.6	75.7	62.0
3-O-ß-D-Glcp	A_α	92.9	71.9	83.3	69.0	72.2	61.6
	$A_ß$	96.6	74.7	85.6	69.1	76.5	61.7
Tetrasaccharide 2							
ß-D-Glcp	D	103.3	74.0	76.3	70.2	76.7	61.4
4-O-ß-D-Glcp	C	103.1	73.6	75.5	79.2	76.2	60.7
4-O-ß-D-Glcp	B	103.4	74.3	75.5	79.2	76.2	60.7
3-O-ß-D-Glcp	A_α	92.7	71.7	83.0	68.8	71.9	61.3
	$A_ß$	96.4	74.8	85.3	68.8	76.7	61.4

TABLE V
^1H NMR vicinal couplings (J, Hz) for the lateral chains of the residues of 1 and 2 in D_2O at 40 °C, and estimated populations of the rotamers *gg* and *gt*,.

$^3J_{H,H}$	Unit								
	2-A_α	2-$A_ß$	2-B	2-C	2-D	1-A_α	1-$A_ß$	1-B	1-C
$J_{5,6S}$	2.3	2.6	2.5	2.4	2.4	2.5	2.6	2.5	2.6
$J_{5,6R}$	5.2	5.1	5.1	5.1	5.1	5.0	5.0	5.1	5.2
%*gg*	60	60	60	60	60	60	60	60	60
%*gt*	40	40	40	40	40	40	40	40	40

namely, DQF-COSY, TOCSY, ROESY (Fig 2), HMQC, and HMBC. The first-order chemical shifts and relevant coupling constants for 1 and 2 are shown in Tables III-V.

Hydroxymethyl conformation. Glucose $H6_{proR}$, $H6_{proS}$ were assigned as previously reported for similar derivatives.[19] The distribution of rotamers was calculated from the first order *J* couplings which could be measured in the 1D spectra of 1 and 2 and from the cross peaks patterns of the DQF-COSY experiment, following well established methodology[20] by using the Karplus-Altona[21] equation (Table V). The observed couplings for the lateral chain of the different glucose residues can be explained for *ca.* 60:40 (±5) distributions of *gg* and *gt* rotamers, which agree with the MD results. The distribution of rotamers indicates that, as previously described,[22] the

tg rotamers of glucopyranoses in water solution do not contribute to the conformational equilibrium. Although these rotamers could be stabilized by an intramolecular hydrogen bond between O-4 and O-6, as observed in MD simulations *in vacuo*,[23] recent quantum chemical calculations of glucose in aqueous solution[24] have shown that the hydroxymethyl equilibrium is controlled by solute-solvent hydrogen bonding interactions and that unfavourable solvation of the *tg* conformer relative to both the *gg* and *gt* rotamers causes its destabilization.

Analysis of NOE data. An important handicap for the NOE-based[25] conformational analysis of the ß(1->4) linkages of oligosaccharides is the problem of severe overlap among H-3, H-4, and in some cases H-3', nuclei with potential or expected NOEs to H-1'. In the case of the compounds presented in this study, H-4 does overlap with H-3 for both ß(1->4) linkages. 2D-ROESY experiments could not alleviate the overlapping problem (Table VI). The problem may be resolved through the use of 2D-HSMQC-ROESY experiments,[26a] which allow detection of NOEs using the carbon frequencies to remove the proton frequency degeneracy. However, due to their correlation times, the smaller NOEs for trisaccharides and tetrasaccharides prompted us to use rotating-frame NOEs to examine the possibility of H-1'-H-4 or H-1'-H-3 dipolar relaxation, but using the non-overlapping C-3 and C-4 ^{13}C NMR frequencies to label the cross-peak. An example of the experiment for compound **1** is given in Figure 3. The presence of cross-peaks H-1''/C-4', H-1''/C-6', H-1''/C-5'', and H-1''/C-3'' can be noted, as well as the intraresidue connectivities H-1'/C-3', H-1'/C-5', H-1/C-3, and H-1/C-5 for the other glucose rings. Therefore, it can be concluded that no important cross-relaxation between H-1'' and H-3' does exist for both ß(1->4) linkages. Besides, the existence of NOE between H-1'' and H-4' and not between H-2''and H-4' implies that both ß(1->4) linkages spend most of their time in the region defined by local minima A, B, C, and C'. However, the differentiation among these geometries is rather difficult since their expected interresidue contacts are very similar. Nevertheless, the presence of NOE between H-1' and the H-6s protons indicate that the region defined by minimum A for the ß(1->4) linkage is populated to some extent. However, the fast equilibrium between the *gg* and *gt* rotamers with a different correlation time to that of the overall motion implies that the exact value of this NOE is rather difficult to simulate quantitatively.[25] An estimation of interresidue distances may be obtained by use of the isolated spin pair approximation (ISPA),[25] using the volumes of the cross peaks between proton pairs in ROESY spectra acquired with a relatively short mixing time (Table VI). No long-range NOEs between non-neighbor glucose moieties were detected in the different experiments performed. The ISPA approximation leads to H-1'''-H-4''(H-1''-H-4') and H-1'-H-3 distances in the range

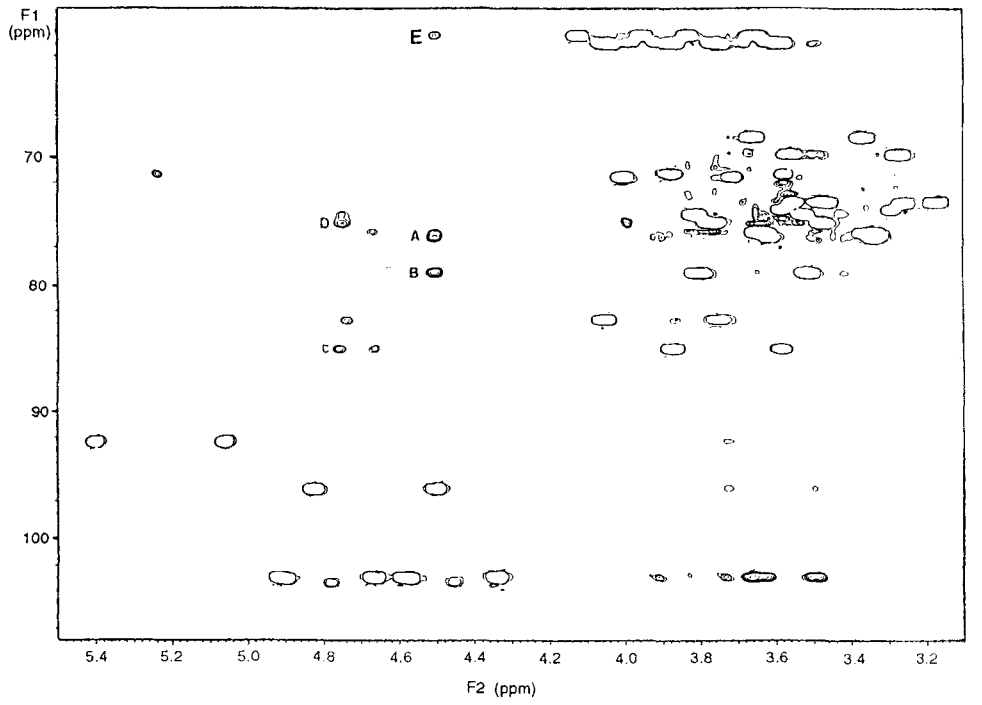

Figure 3. HSMQC-ROESY spectrum of compound **2** in D_2O at 37 °C. Relevant cross-peaks are indicated (A) H-1C/C-3C + C5C, (B) H-1C/C-4B, (C) H-1B/C-3A, (D) H-1B/C-3B + C5B. (E) H-1C/C-6B. No connectivity between H-1C and H-3B or H-5B is detected.

TABLE VI
Experimental 2D-ROESY cross peaks (mix=350 ms) for **1** and **2** at 40 °C in D_2O.

	Cross peak intensity (%)				
Proton Pair	Compound 1	2	Proton Pair	Compound 1	2
H-1'''-H-4''	5	6	H-1'-H-3ß	5	5
H-1'''-H-3'''	7[a]	9[a]	H-1'-H-3'	9[c]	9[c]
H-1'''-H-5'''	7[a]	9[a]	H-1'-H-5'	9[c]	9[c]
H-1'''-H-6''$_R$	*ca.*1	*ca.* 1	H-1'-H-3$_\alpha$	5	5
H-1'''-H-6''$_S$	*ca.*1	*ca.* 1	H-1-H-3ß	3	4
H-1''-H-4'	5	6	H-1-H-5ß	4	5
H-1''-H-3''	7[b]	9[b]	H-1-H-2$_\alpha$	3	4
H-1''-H-6'$_{R,S}$	*ca.*1	*ca.*1	H-1''-H-5''	7[b]	9[b]

a.b.c. Overlapping signals. The addition of both cross-peaks is given.

TABLE VII
Experimental and calculated steady-state NOEs in D_2O upon saturation of H-1'

	Compound		Observed NOE for signal(%) Conformation[c]								
	1	2	A	B	C	D	E	A'	B'	C'	D'
H-1'''-H-4''	3	4	3.2	3.7	4.0						
H-1'''-H-3'''	4[a]	6[b]	2.4	2.8	2.7	2.6	2.5				
H-1'''-H-5'''	4[a]	6[b]	2.3	2.8	2.7	2.7	2.6				
H-1'''-H-6''$_R$	-	-	0.5								
H-1'''-H-6''$_S$	-	-	0.5								
H-1''-H-4'	3	4	3.2	3.7	4.0						
H-1''-H-3''	4[a]	6[b]	2.4	2.8	2.7	2.6	2.5				
H-1''-H-5''	4[a]	6[b]	2.3	2.8	2.7	2.7	2.6				
H-1''-H-6'$_R$	-	-	0.5								
H-1''-H-6'$_S$	-	-	0.5								
H-1'-H-3ß	3	4						2.4	3.3	3.5	0.7
H-1'-H-3'	3	4						2.7	2.7	2.7	2.6
H-1'-H-5'	2	3						2.5	2.6	2.4	2.4
H-1'-H-3$_\alpha$	3	4						2.5	3.3	3.6	0.8
H-1-H-3ß	2	3						2.7	2.7	2.7	2.6
H-1-H-5ß	2	4						2.2	2.6	2.3	2.3
H-1-H-2$_\alpha$	2	4						2.9	2.9	2.9	2.9

a.b. Overlapping signals at 40 °C· c. Full matrix relaxation method, τ_C=0.3*10^{-9} s.

of 2.3-2.4 Å for both ß(1->4)linkages and 2.2-2.3 Å for the corresponding ß(1->3) one, respectively, as expected for the low energy area. With these data, no discrimination among the different conformers is possible, since the distances for the indivual minima included in the main region do not differ substantially from each other.

The corresponding average distance for the ß(1->4)linkages of **2** from the MD simulations is <r>= 2.40 Å, while the corresponding $\langle r^{-6}\rangle^{1/6}$ distance was 2.28 Å which agree with the experimental results. Nevertheless, oscillations between 2.1 and 3.0 Å could be observed. Fairly similar results (<r>= 2.32 Å, $\langle r^{-6}\rangle^{1/6}$ = 2.20 Å) were obtained for the ß(1->3) linkage. The ISPA approximation produces average H-1''-H6's distances in between 3.0 and 3.4 Å, which also are compatible with the low energy region of the cellobiose-type linkage and, as stated above, the presence of this NOE indicate that local minimum A is contributing to the equilibrium. The results of the evaluation of the experimental data *via* a complete relaxation matrix approach[25,27,28] using either a single conformation or an average[29] according to the Boltzmann

distribution function[30] are collected in Table VI. The comparison among the observed and calculated interresidue cross peaks H-1'-H-4 and H-1'-H-$6_{proS,R}$ for the different individual minima (Table VII) showed that a satisfactory match could be obtained by considering the presence of the different conformers A, B, C, and C' of the ß(1->4) linkage in the conformational equilibrium in water, since none of the individual geometries could fit quantitatively all the NOE values simultaneously. Nevertheless, it should be pointed out that it is difficult to establish unequivocally the presence of conformers B and C, although the MD simulations sample those regions significantly. On the other hand, the presence of conformers D or E in an appreciable extent (>5%) can be discarded indeed since they would produce H-1'-H-4 intensities noticeably smaller than those measured along with observable NOE values for the H-1'-H-3 and/or H-2'-H-4 contacts that were never detected either in steady state or HSMQC-ROESY or regular ROESY measurements. These results indicate that the extent of flexibility around the β(1-4) linkage in these compounds in water seems to be rather limited, and can be satisfactorily described by considering contributions of conformers defined by Φ=15±45° and Ψ=-20±30°. On the other hand, there is not possible discrimination between conformers A' or B' of the laminaribiose-type of linkage since both of them satisfy the observed NOEs within experimental error. Since both conformers have also been previously found in computational studies[8] and in the X-ray analysis of different laminaribiose analogues,[9] and also both are sampled during our MD simulations, it seems reasonable to assume the existence of flexibility for this glycosidic linkage and the participation of both local minima in the conformational averaging. Nevertheless, only *ca.* 5-10% of every potential energy surface seems to be populated in water solution as described for different ß(1->3) and ß(1->4) linked oligosaccharides.[7,8] The MD simulations produced average O-5''-O-3' and O-5'-O-4 distances of 3.05±0.20 Å indicating the possible presence of intramolecular hydrogen bond. However, it has to be noted that this hydrogen bond does not seem to be essential to define the shape of these molecules. In fact, previous data for the LeX-type oligosaccharides[31] have shown that their conformations are very similar to those reported in this paper. In fact, although the existence of the O-5´-O-3 hydrogen bond in methyl β-D-cellobioside has been recently demonstrated in DMSO-d_6, there are contradictory results in water since for methyl β-D-cellobioside it has been proposed to dissapear in water solution, at least for most of the time.[16] On the other hand, it has been postulated to exist in 6'-*O*-sialyl lactose.[32] Therefore, the global shape of both compounds **1** and **2** is fairly linear with alternation of the α and β-faces of the glucopyranose rings, although the ß(1->3) linkage could provide a higher source of flexibility.[3c] Stereo views of different possible three dimensional structures of the tetrasaccharide are shown in Fig. 4.

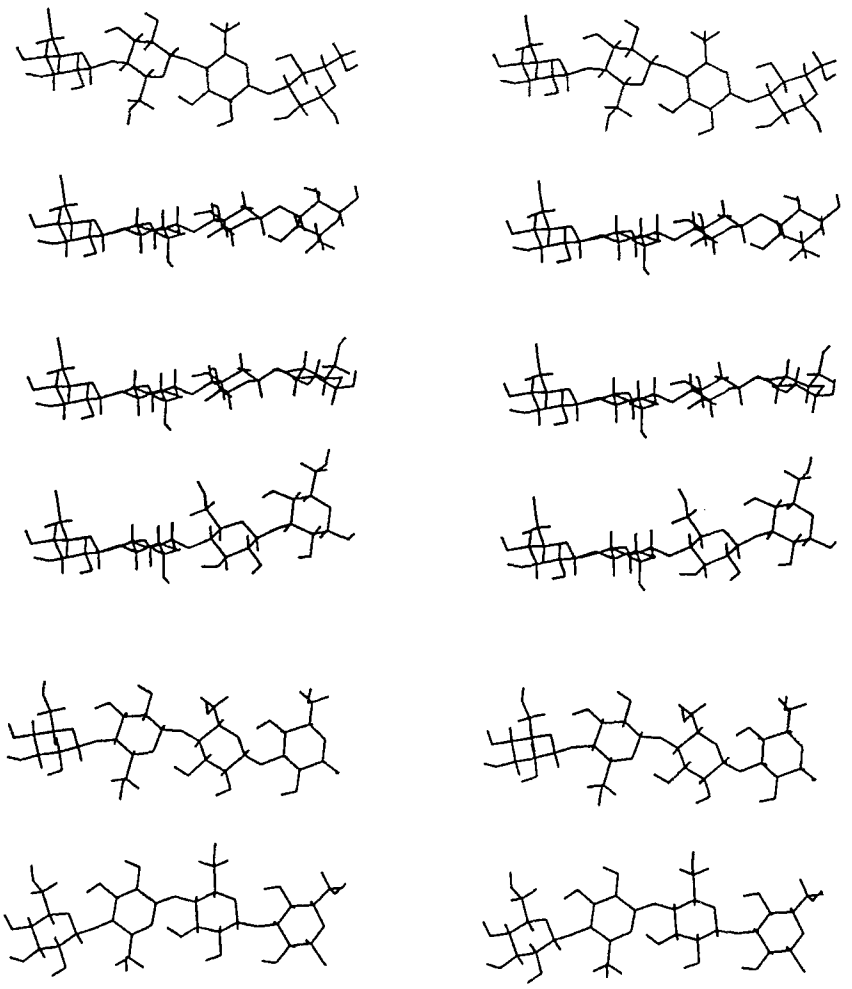

Figure 4. Stereo views of some of the low-energy conformers of compound **2**. Different combinations of local minima A and B for the ß(1->4) glycosidic linkage and of A' and B' for the corresponding ß(1->3) one are shown. In all cases the structure of the tetrasaccharide is fairly linear.

EXPERIMENTAL

Materials. Compounds **1** and **2** were prepared by enzymatic degradation of glucan as previously described.[3]

Nuclear Magnetic Resonance. All the experiments were performed at 30 and 40 °C on a Varian Unity 500 spectrometer. The concentration of the samples was about 20 mM in D_2O solution. The samples were exchanged with D_2O and degassed under argon.

The steady state NOE experiments were performed through the interleaved differential technique using a saturation delay of 7 s. Between 512 and 1024 free induction decays were accumulated for each irradiation site. 2D-ROESY experiments[33] were carried out using mixing times of 300, 400, and 500 ms and were integrated using standard VARIAN software after applying a third order polynomial baseline correction in both dimensions. The pure absorption HSMQC-ROESY experiments[26] were collected in the ^{1}H-detection mode using the pulse sequence 90(^{1}H)-Δ-90(^{1}H,^{13}C) - $t_1/2$ - 180(^{1}H) - $t_1/2$ -90(^{1}H,^{13}C)-Δ-SpinLock-Acq(^{1}H) where Δ is $1/2J_{CH}$ and the Spin Lock time was set to 300 ms. The phase cycling was based on the combination of the original HSMQC[26] and ROESY[33] pulse sequences. A data matrix of 128 * 2K points was used to resolve a spectral width of 8000 Hz and 2000 Hz in F_1 and F_2, respectively. The carrier was set 100 Hz downfield from the most deshielded proton resonance. 256 scans were used per increment with a relaxation delay of 1 s and a Δ delay corresponding to a *J* value of 150 Hz. A BIRD-pulse was use to minimize the proton signals bonded to ^{12}C. ^{13}C-decoupling was not used during acquisition. Prior to Fourier transformation, squared cosine bell functions were applied in both dimensions and zero filling was used to expand the data to 2K * 4K.

Molecular mechanics and dynamics calculations. All the previously described low energy conformers of cellobiose[7,8] and laminaribiose[8] were used to build different conformers of the ß-tetrasaccharide **2**, as its methyl glycoside, and submitted to further minimization using the CVFF[34] and AMBER[35] force fields. Due to the similar NMR parameters found for trisaccharide **1** (see below), it was assumed that this compound adopts a similar solution conformation. Glycosidic torsion angles at the (1->4) linkages are defined as Φ_{H3} H-1'''-C-1'''-O-1'''-C-4'', Ψ_{H3} C-1'''-O-1'''-C-4''-H-4'', and Φ_{H2} H-1''-C-1''-O-1''-C-4', Ψ_{H2} C-1''-O-1''-C-4'-H-4', (using proton as reference), or as Φ_3 O-5'''-C-1'''-O-1'''-C-4'', Ψ_3 C-1'''-O-1'''-C-4''-C-5'', and Φ_2 O-5''-C-1''-O-1''-C-4', Ψ_2 C-1''-O-1''-C-4'-C-5', (using a heavy atom as reference). On the other hand, that at the ß(1->3) is defined as Φ_{H1} H-1'-C-1'-O-1'-C-3 and Ψ_{H1} C-1'-O-1'-C-3-H-3 or as Φ_1 O-5'-C-1'-O-1'-C-3 and Ψ_1 C-1'-O-1'-C-3-C-4. For all torsion angles, $\Phi = \Phi_H$-120°, $\Psi = \Psi_H$-120°. A dielectric constant of 78 D was used for the CVFF calculations, while a distance dependent dielectric constant was employed for the AMBER minimizations. The torsion angle values for the different local minima A-E when using either the AMBER or the CVFF force fields did not differ more than 10°. Their corresponding populations were calculated from the energy steric values for the corresponding local minima, neglecting entropic effects. Several minimized geometries were then taken as starting structures for Molecular Dynamics

calculations (MD) *in vacuo* by using the same force fields as integrated in the Discover 2.8 program.[36] The MD simulations were performed at 313 °K with a time step of 1 fs. The total simulation time was 500 ps or 1 ns. Trajectory frames were saved every 0.5 or 1 ps. The trajectories were then examined with the Analysis module of INSIGHT II.[37] The steady state 1D-NOE were calculated according to the complete relaxation matrix method[38] by using the NOEMOL program[39] for the proton coordinates of the different conformers and for their Boltzmann distribution, calculated from the AMBER relative energies at 40 °C. Isotropic motion and no external relaxation was assumed in the calculation process. Since NOEs are extremely dependent on the correlation time, different τ_C values were used in order to get the best match between the experimental and the calculated NOE for H-1'-H-3' and H-1'-H-5' proton pairs. A satisfactory match was found by using τ_C=0.3 ns. 2D-ROESY experiments were used to estimate interproton distances according to the isolated spin pair approximation.[25] Different mixing times were used in order to test the occurrence of spurious Hartmann-Hahn effects.

ACKNOWLEDGEMENTS

We thank Dr. M. Forster (Potters Bar, UK) for the use of the NOEMOL programme, Dr. U. Heinemann (Freie Universität Berlin) for a preprint of reference 4 prior to publication, and Dr. A. Imberty (Nantes, France) for a preprint of reference 12 prior to publication. Funding from DGICYT (grant PB-870367) and MEC (BIO91-0477) is gratefully acknowledged.

REFERENCES

1. (a) F. W. Parrish, A. S. Perlin and E. T. Reese, *Can. J. Chem.*, **38**, 2094 (1960). (b) J. R. Woodward, G. B. Fincher and B. A. Stone, *Carbohydr. Polym.*, **3,** 207 (1983). (c) 37 G. S. Buliga, D. A. Brant and G. B. Fincher, *Carbohydr. Res.*,**157,** 139 (1986).

2. (a) T. Godfrey in *Industrial Enzymology*; T. Godfrey and J. Reinchelt, Eds.; MacMillan: London, 1983, p 466.

3. C. Malet, J. Jiménez-Barbero, M. Bernabé, C. Brosa and A. Planas, *Biochem. J.,* in press.

4. T. Keitel, O. Simon, R. Borris and U. Heinemann, *Proc. Natl. Acad. Sci. USA*, **90,** 5287 (1993).

5. (a) P. B. Høj, E. B. Rodríguez, R. V. Stick and B. A. Stone, *J. Biol. Chem.*, **264**, 4939 (1989). (b) P. B. Høj, R. Condron, J. C. Traeger, J. C. McAuliffe and B. A. Stone, *J. Biol. Chem.*, **267**, 25059 (1992).

6. K. Bock, J. O. Duus, B. Norman and S. Pedersen, *Carbohydr. Res.*, **211**, 219 (1991).

7. (a)A. D. French, V. H. Tran and S. Perez, *ACS Symp. Ser.*, **430**, 191 (1990), and references therein. (b) T. Peters, B. Meyer, R. Stuike-Prill, R. Somorjai and J.R. Brisson, *Carbohydr. Res.*, **238**, 49 (1993), and references therein.

8. M. K. Dowd, A. D. French and P. J. Reilly, *Carbohydr. Res.*, **223**, 15 (1992).

9. (a) S. S. C. Chu and G. A. Jeffrey, *Acta Crystallogr.*, ***B*** **24**, 830 (1968). (b) J. T. Ham and D. G. Williams, *Acta Crystallogr.*, ***B*** **26**, 1373 (1970). (c) H. Takeda, N. Yasuoka and N. Kasai, *Carbohydr. Res.*, **53**, 137 (1977). (d) K. Noguchi, K. Okuyama, S. Kitamura and K. Takeo, *Carbohydr. Res.*, **237**, 33 (1992).

10. A. Rivera-Sagredo, D. Solis, T. Diaz-Mauriño, J. Jiménez-Barbero and M. Martín-Lomas, *Eur. J. Biochem.*, **197**, 217 (1991).

11. M. Bernabé, A. Fernández-Mayoralas, J. Jiménez-Barbero, M. Martín-Lomas and A. Rivera-Sagredo, *J. Chem. Soc. Perkin Trans II*, 1867 (1989).

12. (a) Y. Bourne, P. Rouge and C. Cambillau, *J. Biol. Chem.*, **267**, 197 (1992). (b) A. Imberty, Y. Bourne, C. Cambillau, P. Rouge and S. Perez, *Adv. Biophys. Chem.*, in press.

13. (a) S. W. Homans, *Biochemistry*, **29**, 9110 (1990)(b) S. W. Homans and M. Forster, *Glycobiology*, **2**, 143 (1992). (c) J. N. Scarsdale, P. Ram, J. H. Prestegard and R. K. Yu, *J. Comput. Chem.*, **9**, 133 (1988). (c) B. J. Hardy and A. Sarko, *J. Comput. Chem.*, **14**, 831 (1993). (d) B. J. Hardy and A. Sarko, *J. Comput. Chem.*,**14**, 848 (1993).

14. I. Tvaroska and T. Bleha, *Adv. Carbohydr. Chem. Biochem.*, **47**, 45 (1989).

15. (a) H. C. Siebert, G. Reuter, R. Schauer, C. W. von der Lieth and J. Dabrowski, *Biochemistry*, **31**, 6962 (1992). (b) A. E. Aulabaugh, R. C. Crouch, G. E. Martin, A. Ragouzeos, J. P. Shockcor, T. D. Spitzer, R. D. Farrant, B. D. Hudson and J. C. Lindon, *Carbohydr. Res.*, **230**, 201 (1992).

16. L. M. J. Kroon-Batenburg, J. Kroon, B. R. Leeflang, and J. F. G. Vliegenthart, *Carbohydr. Res.*, **245**, 21 (1993).

17. K. Bock, *Pure Appl. Chem.*, **55**, 605 (1983).

18. B. Meyer, *Topics Curr. Chem.*, **154**, 141 (1990).

19. Y. Nishida, H. Ohrui and H. Meguro, *Tetrahedron Lett.*, **25**, 1575 (1984).

20. Y. Nishida, H. Hori, H. Ohrui and H. Meguro, *J. Carbohydr. Chem.*, **7**, 239 (1988).

21. C. A. G. Haasnoot, F. M. de Leeuw, and C. Altona,*Tetrahedron*, **36**, 2783 (1980).

22. B. R. Leeflang, J. F. G. Vliegenthart, L. M. J. Kroon-Batenburg, B. P. van Eijck and J. Kroon, *Carbohydr. Res.*, **230**, 41 (1992).

23. L. M. J. Kroon-Batenburg and J. Kroon, *Biopolymers*, **29**, 1243 (1990).

24. C. J. Cramer and D. G. Truhlar, *J. Am. Chem. Soc.*, **115**, 5745 (1993).

25. D. Neuhaus and M. P. Williamson, *The Nuclear Overhauser Effect in Structural and Conformational Analysis* (1989) VCH Publishers, NY.

26. (a) P. Fernández and J. Jiménez-Barbero, *J. Carbohydr. Chem.* in press. (b)E. R. P. Zuiderweg, *J. Magn. Reson.*, **67**, 565 (1990).

27. J. R. Brisson and J. P. Carver, *Biochemistry*, **22**, 1362 (1983).

28. D. A. Cumming and J. P. Carver, *Biochemistry*, **26**, 6664 (1987).

29. K. Bock, H. Lönn and T. Peters, *Carbohydr. Res.*, **198**, 375 (1990).

30. A. Imberty, V. Tran and S. Perez, *J. Comput. Chem.*, **11**, 205 (1989).

31. K. E. Miller, C. Mukhopadhyay, P. Cagas and C. A. Bush, *Biochemistry*, **31**, 6703 (1992), and references therein.

32. L. Poppe, R. Stuike-Prill, B. Meyer and H. van Halbeek, *J. Biomol. NMR*, **2**, 109 (1992).

33. (a)A. A. Bothner-By, R. L. Stephens, J.-M. Lee C. D. Warren and R. W. Jeanloz, *J. Am. Chem. Soc.*, **106**, 811 (1984). (b) A. Bax and D. G. Davis, *J. Magn. Reson.*, **63**, 207 (1985).

34. A. T. Hagler, S. Lifson and P. Dauber. *J. Am. Chem. Soc.*, **101**, 5122 (1979).

35. S. J. Weiner, P. A. Kollman, D. A. Case, U. C. Singh and C. Ghio, *J. Am. Chem. Soc.*, **106,** 765 (1984).

36. Discover 2.8 Program. *Biosym Technologies Inc.* San Diego, CA.

37. Insight 2.1.0 Program. *Biosym Technologies Inc.* San Diego, CA.

38. T. Peters, J.R. Brisson and D. R. Bundle, *Can. J. Chem.*, **68,** 979 (1990), and references therein.

39. (a) M. Forster, C. Jones and B. Mulloy, *J. Mol. Graph,* **7**, 196 (1989). (b) M. J. Forster, *J. Comput. Chem.* **12**, 292 (1991).